AIP Applied Physics Letters

Deformation behaviors of InP pillars under uniaxial compression

Sheng-Rui Jian, T.-H. Sung, J. C. Huang, and Jenh-Yih Juang

Citation: Applied Physics Letters **101**, 151905 (2012); doi: 10.1063/1.4758479
View online: http://dx.doi.org/10.1063/1.4758479
View Table of Contents: http://scitation.aip.org/content/aip/journal/apl/101/15?ver=pdfcov
Published by the AIP Publishing

Articles you may be interested in
Determination of stress, strain, and elemental distribution within In(Ga)As quantum dots embedded in GaAs using advanced transmission electron microscopy
Appl. Phys. Lett. **102**, 173115 (2013); 10.1063/1.4804380

Plastic deformation of gallium arsenide micropillars under uniaxial compression at room temperature
Appl. Phys. Lett. **90**, 043123 (2007); 10.1063/1.2432277

Synthesis of InN/InP core/sheath nanowires
Appl. Phys. Lett. **84**, 1546 (2004); 10.1063/1.1651331

Yield strength and dislocation mobility in plastically deformed bulk single-crystal GaN
J. Appl. Phys. **90**, 6539 (2001); 10.1063/1.1415754

Mechanical deformation of InP and GaAs by spherical indentation
Appl. Phys. Lett. **78**, 3235 (2001); 10.1063/1.1372207

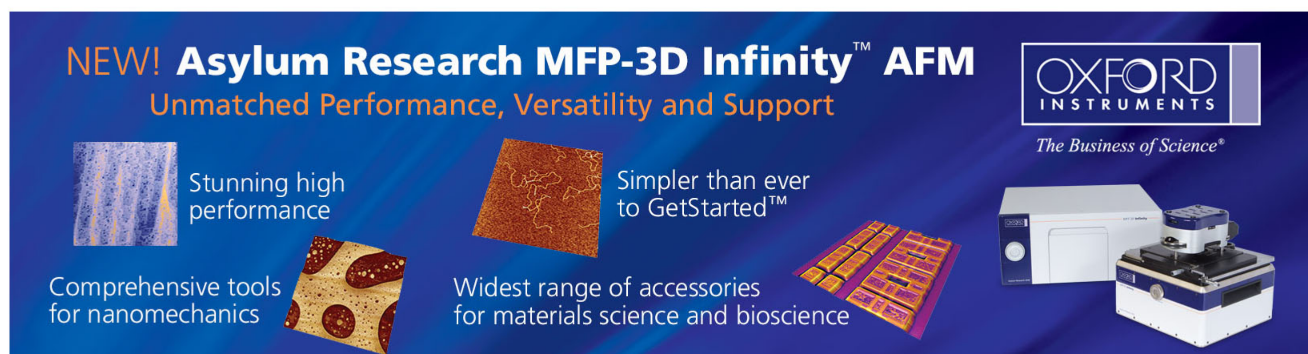

This article is copyrighted as indicated in the article. Reuse of AIP content is subject to the terms at: http://scitation.aip.org/termsconditions. Downloaded to IP: 140.113.38.11 On: Thu, 01 May 2014 08:29:12

Deformation behaviors of InP pillars under uniaxial compression

Sheng-Rui Jian,[1,a)] T.-H. Sung,[2] J. C. Huang,[2] and Jenh-Yih Juang[3]
[1]*Department of Materials Science and Engineering, I-Shou University, Kaohsiung 840, Taiwan*
[2]*Department of Materials and Optoelectronic Science, National Sun Yat-Sen University, Kaohsiung 804, Taiwan*
[3]*Department of Electrophysics, National Chiao Tung University, Hsinchu 300, Taiwan*

(Received 4 August 2012; accepted 27 September 2012; published online 9 October 2012)

We report the deformation behavior of single-crystal InP(100) micropillars, measuring about 1 μm in diameter and 2 μm in height, subjected to uniaxial compression at room temperature. The engineering stress-strain results indicated that the yield strength of InP pillar is about 2.5 GPa, and the presence of a drastic strain burst right after yielding. Cross-sectional transmission electron microscopy microstructural observations reveal the formation of extremely dense twins. The results indicate that the plastic deformation in InP micropillars is dominated by explosive generation of deformation twins under the high stress state. © *2012 American Institute of Physics*. [http://dx.doi.org/10.1063/1.4758479]

Understanding the dislocation-based plasticity in prominent functional materials at the sub-micron scale is important not only for gaining insights into the fundamental mechanisms of small scale plasticity but also for designing reliable devices in the field of nano- or micro-electromechanical systems. Recent advancement in nanoscale fabrication and mechanical measurements has enabled the systematic investigation of size effects on the deformation behaviors of various materials. In this way, the size-scale effects on the materials mechanics can be explored under the conditions of minimized imposed deformation gradients, thus, limiting influence from concomitant changes in local strength and hardening rate resulted from the evolution of geometrically necessary dislocations induced by strain gradients.[1] Indeed, the compression tests on micro-pillars made of various materials[1–4] have been demonstrated to exhibit dramatically different deformation behaviors as compared to their bulk counterparts. For instance, in addition to prevailing the tenet of "smaller is stronger" in essentially all the measurements preformed, drastic reduction in brittle-to-ductile transition temperatures in micro-compression of GaAs[5,6] and Si[7] was also observed when the diameter of the testing pillars is smaller than certain critical sizes.

However, because of the small sizes of the structures, observation and subsequent analysis remain as challenging tasks and even involve numerous assumptions. To address this issue, micro-compression tests on pillars made of various materials have been conducted and analyzed with the aids of transmission electron microscopy (TEM) to delineate the activities of the extended defects associated with the compression-induced deformation.[3–9] Very recently, *in-situ* micro-compression test on Al micro-pillars has been conducted directly inside a high-resolution electron microscope.[10] This enables the *in-situ* observations of the structural changes during compression test and provides information concerning the mechanisms governing the manifestations of deformation behaviors, including the instant and location of the initiation of shear bands, cracks, or dislocations.

In practice, a basic micro-compression test consists of uniaxial compression on micro/nano-sized pillars that are usually prepared by means of focused ion beam (FIB) milling. Micro/nanopillars were directly carved into the surface of a substrate material by FIB milling. Once the micro/nanopillars are fabricated, a modified nanoindentation system equipped with a flat-end diamond indenter is used for carrying out the micro-compression measurements. During the engagement of the indenter, the micropillars protruding from the substrate have the first contact with the indenter tip and are compressed afterwards. The load-displacement data are then continuously recorded in the same way as being practiced in nanoindentation measurements.[4] The load-displacement data can also be directly converted into the engineering stress-strain responses of pillars by dividing the applied load with the cross-sectional area and the apparent displacement with the effective gauge length of pillars, respectively.

Nucleation of dislocations can occur homogeneously in the bulk as full dislocation loops, or occur heterogeneously at surfaces and edges as half or quarter dislocation loops. In nanoindentation tests, the stress state is non-uniform and the resolved shear stress on potential slip systems reaches a maximum in regions directly underneath the contact. Therefore, dislocation nucleation is expected to occur inside the solid. In micropillar compression tests, on the other hand, the stress field is in principle uniform and dislocation nucleation can occur anywhere within the gauge section, including at the free surfaces and edges. This stress-state difference is crucial in understanding the deformation behaviors and the relevant mechanisms deduced from nanoindentation or micropillar compression tests. Herein, in this study, we experimentally studied the deformation behaviors of single-crystal (100)-plane-oriented InP pillars under uniaxial compression. InP has the face-centered cubic (zincblende) crystal structure. The cross-sectional TEM (XTEM) observations combined with the selected area diffraction (SAD) analyses indicate that twinning is the predominant deformation mechanism in micron-sized InP pillars under compression. The results

[a)]Author to whom correspondence should be addressed. Electronic address: srjian@gmail.com. Tel.: +886-7-6577711 ext. 3130.

 © 2012 American Institute of Physics

This article is copyrighted as indicated in the article. Reuse of AIP content is subject to the terms at: http://scitation.aip.org/termsconditions. Downloaded to IP: 140.113.38.11 On: Thu, 01 May 2014 08:29:12

clearly exhibited distinctly different stress-induced deformation behaviors as compared to those observed in nanoindentations performed on similar single-crystal InP(100) substrates.[11,12]

The single-crystal (100)-oriented InP substrates used in this study are similar to those used previously in nanoindentation tests.[12] The InP micro-pillars were prepared using the dual-beam FIB systems (FIB, SMI 3050 station with Ga ions at 30 keV), following the method developed by Uchic *et al.*[1] The Ga-ion beam operated at a voltage of 30 keV with a beam current of 7–12 nA was initially directed perpendicular to the surface of the InP wafer to mill a cylindrical mesa situating at the middle of a crater about 35 μm in diameter and 1 μm in depth. The same voltage and smaller currents of 0.7–0.09 nA were used to refine to the structure into pillar with targeted height and diameter. The micropillars prepared in this study typically are measured about 1 μm in diameter and around 2 μm in height. However, due to the profile of the Ga-ion beam, the obtained micropillars appear to have a slight taper angle around 1.3°. The inset of Fig. 1(c) shows the typical appearance of the micropillars used in this study prior to compression tests. The thickness of the damaged layers resulted from the side radiation of Ga-ions in the current FIB-milled 1 μm micropillars is estimated to be around 50 nm, and is considered to have negligible effects on the results of the compression tests.

The micropillars are loaded with a uniaxial compression by using the flat-punch Berkovich tip in a commercially available nanoindentation systems (MTS Nanoindenter XP) operating with the continuous stiffness measurement (CSM) function. The tests were carried out with the constant displacement rate mode at a strain rate of 10^{-3} s^{-1}. In order to trace the mechanical response of the pillar at different straining stages, the preset stop displacement was set to be 200 nm. The outside appearance of the as prepared and deformed micropillars was examined by scanning electron microscopy (SEM). The XTEM samples were prepared from the post-compression InP pillars by using a dual-beam FIB (Nova 220) station with Ga ions at 30 keV. The TEM foils were coated with a thin carbon layer for protection. The thickness of the foils is less than 50 nm. The XTEM thin foil specimens were examined in a FEI TECNAI G^2 TEM operating at 200 kV.

Figure 1(a) shows the load-displacement curve for the compression test on InP pillar shown in the inset of Fig. 1(c). The converted engineering stress-strain response of the compressed InP pillar using the method described above is presented in Fig. 1(b). It is evident that initially the micropillars were deformed elastically up to a strain of about 7.6%, and then followed by a drastic strain burst at an apparent yield strength of ~2.5 GPa.

Furthermore, an approximate formula usually used for extracting the Young's modulus of the pillar (E_{pillar}) is employed to obtain the Young's modulus of the present InP pillars by assuming that the applied stresses are uniformly distributed over the entire cross-section of the pillar,[14] as following:

$$E_{pillar} = \left(1 + \frac{\pi D (1 - v)}{8H}\right) \left[\frac{4PH}{\pi D (D + 2H \tan\theta) d}\right], \quad (1)$$

where v, P, d, H, D, and θ are denoted as the Poisson's ratio of InP, the compressive load applied on the pillar, the total displacement of pillar upon compression, the height of pillar, the top diameter of pillar, and the taper angle, respectively. With Eq. (1), the Young's modulus of InP pillars is estimated to be approximately 73.7 ± 3.1 GPa, which is in good agreement with the values obtained by nanoindentation, namely ~82 GPa[11] and 78.9 ± 3.7 GPa,[12] respectively.

However, although GaAs and InP have been shown to exhibit almost the same deformation behaviors in the indentation tests,[11,12] it is noted that the deformation behaviors

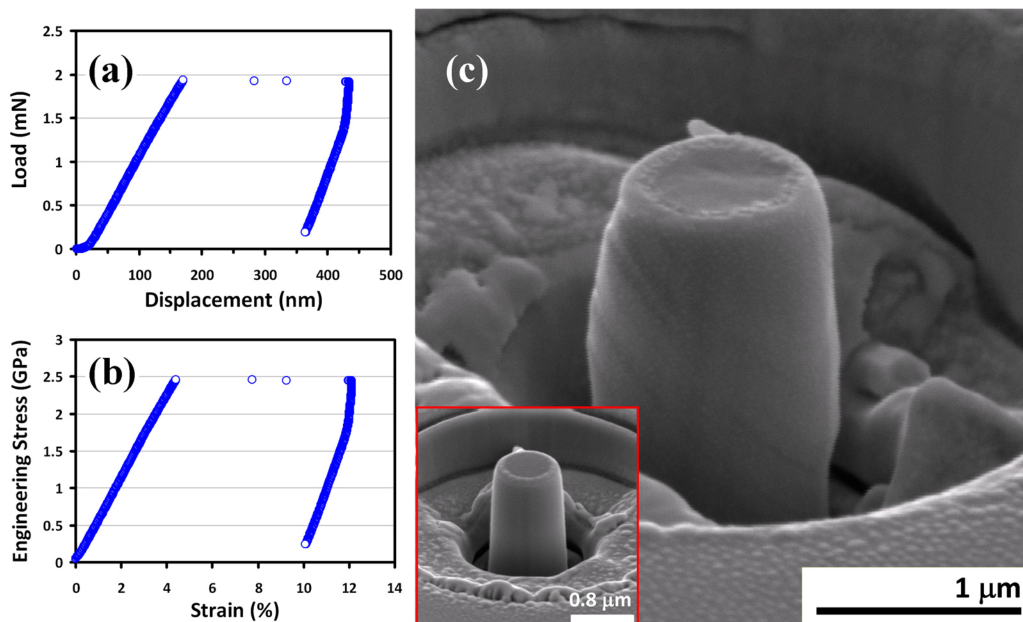

FIG. 1. (a) Load-displacement curve and (b) the engineering stress-stain curve of compression test on InP pillar. (c) SEM images show the compressed InP pillar, and the slip bands are observed on InP pillar. The inset shows the un-compressed InP pillar.

This article is copyrighted as indicated in the article. Reuse of AIP content is subject to the terms at: http://scitation.aip.org/termsconditions. Downloaded to IP: 140.113.38.11 On: Thu, 01 May 2014 08:29:12

displayed in Figs. 1(a) and 1(b) are in sharp contrast to those observed in previous micro-compressions on GaAs pillars with similar sizes,[5] where the yield strength (~2.3 GPa) was clearly indentified and the subsequent flow stress was fluctuating substantially within the range of 1.6–2.6 GPa with no catastrophic strain burst.

The TEM investigations on those GaAs pillars have indicated that, in addition to significant dislocation slips on {111} planes, high density twins as well as microcracks were generated during the micro-compression tests. Therefore, it was suggested[5] that the deformation behaviors of GaAs micro-pillars might have involved different combinations of the above mentioned activities at various deformation stages. On the other hand, the essentially single catastrophic deformation behavior in InP has been attributed to the truncation of either the ability to multiply dislocations or the number of dislocation sources in the pillar.[1,10] It is thus interesting to explore the underlying mechanism that could lead to the apparent differences between the present observations and previous results.

In compression tests carried out under displacement control mode, similar strain burst behaviors have been observed in the micropillars made of hexagonal close-packed GaN[4] and ZnO[13] when the applied load exceeds the yield strength. For all the InP, GaN, and ZnO micropillars, inhomogeneous deformation has occurred, as seen in Fig. 1(c). A closer look at the SEM photograph shown in Fig. 1(c) indicates that this inhomogeneous deformation may have been resulted from the slip bands asymmetrically localized in the gauge range of the deformed pillars. The angle between the inclined slip planes has the angle about 55° with respect to the horizontal (100) plane, suggesting that the slip plane is (111) which should oriented at 54.7° with (111) for cubic crystals.

This phenomenon can be understood as followings. When slip occurred, material was transported from the top pillar surface to the side surfaces. However, dislocation pile-up may form at the intersections preventing further flow across the pillar when the glide bands are intersected. Dislocation pile-up would form along {111} slip planes, therefore, imposes a lateral force on the pillar below the glide band intersection.[7] Nevertheless, whether the result shown in Fig. 1(c) is simply due to collectively activation of existing dislocations or is originated from explosive and highly correlated dislocation generation[10] remains to be clarified.

Figure 2 shows the bright-field XTEM image of the post-compressed InP pillar. It is evident that the contrast bands, as well as the associated diffraction pattern, align at an angle of ~54.7° with respect to the (100) plane, confirming the (111) glide planes. Furthermore, as indicated by the arrow shown in the inset of Fig. 2, the glide planes are apparently terminating at the amorphous surface layer, induced by the damage of FIB beam. This amorphous surface layer in InP is about 50 nm-thick, much thicker than the 5 nm for metallic glass or 10 nm for GaN. Note that the etching rate of InP by FIB is about five times than GaN or ZnO, suggesting InP is more likely to be damaged. For compressions exerted along the $\langle 100\rangle$ direction, the Schmid factor for the $\{111\}\langle 110\rangle$ slip system is calculated to be about 0.41. Under the assumption of a perfectly uniaxial stress throughout the InP pillar, the resolved shear stress (τ_{rss}) on the {111} planes becomes ~1 GPa (2.5 GPa × 0.41), which is substantially smaller than the nanoindentation-derived values of critical resolved shear stress (τ_{crss} ~ 2.8–3.5 GPa) for activating dislocation slip in InP crystals,[15] thus, is consistent with twin-dominated deformation behavior. Similar behavior has been observed in GaAs by Androussi *et al.*[16] It was pointed out that, for fcc structured semiconductors under the high-stress compression condition, the micro-twinning produced by gliding of partial dislocations might become the dominant plastic deformation mechanism over the gliding of perfect dislocations.[16] We believe that similar scenario might also apply for the deformation of the present InP pillars. Indeed, the TEM dark-field image shown in Fig. 3(a), using the $(\bar{1}1\bar{1})_t$ diffraction twin spot in the [011] zone-axis SAD pattern (SADP) in Fig. 3(b), evidently shows the existence of extremely fine twinning lying parallel in the {111} planes. Nevertheless, it is worthwhile to indicate here that although the τ_{crss} values for the hexagonal structured GaN[4] and ZnO[13] are even higher than those of their fcc counterparts, namely InP and GaAs,[5,16] the deformation characteristics were predominantly associated with dislocation activities. The reason

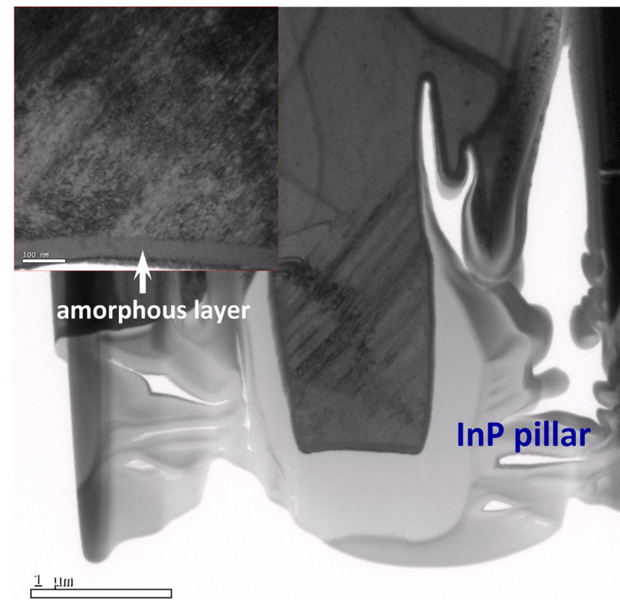

FIG. 2. XTEM bright-field image of InP pillar compressed to a preset displacement 200 nm. The inset shows a magnification of amorphous layer in the upper part of InP pillar.

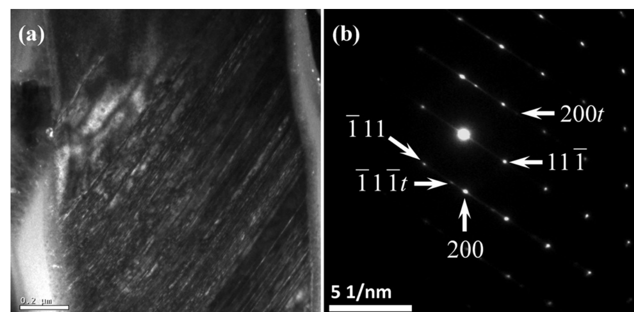

FIG. 3. (a) A close-up view of XTEM dark-field image of compressed InP pillar, showing that the dense twin and (b) the SAD pattern, and the sample is oriented along the [011] zone axis.

This article is copyrighted as indicated in the article. Reuse of AIP content is subject to the terms at: http://scitation.aip.org/termsconditions. Downloaded to IP: 140.113.38.11 On: Thu, 01 May 2014 08:29:12

TABLE I. Comparison of the crystal structure, mechanical data, and dominant deformation modes in the four optoelectronic materials.

	InP[a]	GaAs[5]	ZnO[13]	GaN[4]
Crystal structure	Cubic	Cubic	Hexagonal	Hexagonal
Pillar horizontal plane	(100)	(100)	(0001)	(0001)
Young's modulus, E_{pillar} (GPa)	74	123	123	226
Hardness (GPa)	5	8	7	15
Yield stress (GPa)	2.5	1.8	3	10
Microcompression, τ_{rss} (GPa)	1	0.6–0.9	1.2	4.1
Nanoindentation, τ_{crss} (GPa)[15]	2.8–3.5	4.1–5.2	3.2–4.4	7.6–9.4
Deformation mode	Twinning	Twinning	Dislocation	Dislocation
Shear plane	(111)	(111)	(10–10)	(10–10)

[a]Present work.

for this is not clear at present and certainly requires further studies. A detailed comparison of the deformation characteristics with the prominent mechanical parameters collected from the literature for the above-mentioned compound semiconductors is displayed in Table I.

The strong intensity of the twin spots in the SADP further indicates that the density of the stress-induced twins can be very high. The diffraction spots of the twins are slightly elongated because the twins are essentially consisting of very thin crystalline plates owing to the explosive generation of twins that eventually leads to the drastic strain burst observed in Fig. 1(b). In addition, there is no indication of the formation of cracks or other phases, thus, the deformation behavior in the present case seems to proceed predominantly by the formation and propagation of twins. To give a simple estimation on the number of twins, the energies before and after a twin has traversed the pillar at an angle of 54.7° (Figs. 2 and 3(a)) are compared. Thus, the formation energy (E_f) of a twin in the pillar is approximated by

$$E_f = (\cos 54.7^\circ) \cdot (\pi r^2) \cdot \Gamma, \qquad (2)$$

with r being the radius of pillar and Γ being the energy per unit area of twin, respectively. Taking $\Gamma = 18 \times 10^{-3}$ J/m^2,[17] the number of twins formed can be estimated from the complete release of elastic strain energy. From Fig. 1(a), the elastic strain energy is estimated to be around 1.7×10^{-10} J. Assuming this elastic strain energy is solely related to the formation of twins, we obtain that the number of twins generated by this process is approximately 2×10^3. A higher number of 6×10^3 twins are obtained if the total dissipation energy (i.e., the entire area between the loading and unloading curves shown in Fig. 1(a)) is taken into account for the formation of twins. Such estimation provides the upper limit of the number of twins can be generated within a micro-scale pillar. However, since the unloading may give rise to a small relaxation of the twin structure, the final configuration of the deformation twins should be stabilized by the residual strain remaining in the compressed pillar. In any case, if we assume that the deformation twins are spreading uniformly over the 2 μm gauge length, the average spacing between the twins should be in the order of 0.3–1 nm.[18] Unfortunately, the resolution of Fig. 3(a) appears to be inadequate to give a conclusive account for this estimation and further investigations are certainly needed.

In summary, we reported the results of the room-temperature stress-induced plastic deformation behaviors in single-crystal InP(100) micropillars. The micropillars were fabricated by using the dual-beam focus-ion-beam milling technique and the deformation behaviors were investigated using the micro-compression carried out in a modified nano-indentation facility in combination with the microstructure analyses using cross-sectional transmission electron microscopy. Results reveal that the yield strength of InP micropillars is about 2.5 GPa. A dramatic strain burst is followed by the yielding. Extensive shear sliding occurs along the (111) planes, resulting a Schmid factor of 0.41 and shear stress of ~1 GPa. TEM microstructure analyses confirmed that twinning is the predominant deformation mechanism in the compressed InP pillars.

This work was partially supported by the National Science Council of Taiwan, under Grant Nos. NSC100-2221-E-214-024 and NSC101-2221-E-214-017. J.Y.J. is partially supported by the NSC of Taiwan and the MOE-ATU program operated at NCTU.

[1]M. D. Uchic, D. M. Dimiduk, J. N. Florando, and W. D. Nix, Science **305**, 986 (2004).
[2]S. M. Han, M. A. Phillips, and W. D. Nix, Acta Mater. **57**, 4473 (2009).
[3]Y. H. Lai, C. J. Lee, Y. T. Cheng, H. S. Chou, H. M. Chen, X. H. Du, C. I. Chang, J. C. Huang, S. R. Jian, J. S. C. Jang, and T. G. Nieh, Scr. Mater. **58**, 890 (2008).
[4]T. H. Sung, J. C. Huang, J. H. Hsu, and S. R. Jian, Appl. Phys. Lett. **97**, 171904 (2010).
[5]J. Michler, K. Wasmer, S. Meier, F. Östlund, and K. Leifer, Appl. Phys. Lett. **90**, 043123 (2007).
[6]F. Östlund, P. R. Howie, R. Ghisleni, S. Korte, K. Leifer, W. J. Clegg, and J. Michler, Philos. Mag. **91**, 1190 (2011).
[7]F. Östlund, K. Rzepiejewska-Malyska, K. Leifer, L. M. Hale, Y. Tang, R. Ballarini, W. W. Gerberich, and J. Michler, Adv. Funct. Mater. **19**, 2439 (2009).
[8]E. A. Withey, A. M. Minor, D. C. Chrzan, J. W. Morris, Jr., and S. Kuramoto, Acta Mater. **58**, 2652 (2010).
[9]R. J. Milne, A. J. Lockwood, and B. J. Inkson, J. Phys. D: Appl. Phys. **44**, 485301 (2011).
[10]Z. J. Wang, Q. J. Li, Z. W. Shan, J. Li, J. Sun, and E. Ma, Appl. Phys. Lett. **100**, 071906 (2012).
[11]J. E. Bradby, J. S. Williams, J. Wong-Leung, M. V. Swain, and P. Munroe, Appl. Phys. Lett. **78**, 3235 (2001).
[12]S. R. Jian and J. S. C. Jang, J. Alloys Compd. **482**, 498 (2009).
[13]T. H. Sung, J. C. Huang, J. H. Hsu, S. R. Jian, and T. G. Nieh, Appl. Phys. Lett. **100**, 211903 (2012).
[14]Y. Yang, J. C. Ye, J. Lu, F. X. Liu, and P. K. Liaw, Acta Mater. **57**, 1613 (2009).
[15]J. E. Bradby, J. S. Williams, and M. V. Swain, J. Mater. Res. **19**, 380 (2004).
[16]Y. Androussi, G. Vanderschaeve, and A. Lefebvre, Philos. Mag. A **59**, 1189 (1989).
[17]T. Duffar and A. Nadri, Scr. Mater. **62**, 955 (2010).
[18]Since the "twinning" appears to concentrate mainly on the bulged region, our estimation by assuming a 2 μm gauge length is, thus, only representing a lower bound value for the twin density.

This article is copyrighted as indicated in the article. Reuse of AIP content is subject to the terms at: http://scitation.aip.org/termsconditions. Downloaded to IP: 140.113.38.11 On: Thu, 01 May 2014 08:29:12